Adsorption of plasma proteins on polyethylene oxide-modified lipid bilayers studied by total internal reflection fluorescence

Zhong Xu[a], Roger E. Marchant[a,b],*

[a]*Department of Biomedical Engineering, Case Western Reserve University, Wickenden Building, Cleveland, OH 44106, USA*
[b]*Department of Macromolecular Science, Case Western Reserve University, Wickenden Building, Cleveland, OH 44106, USA*

Abstract

Distearoylphophatidylcholine (DSPC) mixed with various mole percentages of polyethylene oxide (number average molecular weight 2000)-grafted distearoylphosphatidylethanolamine (PEO2000-DSPE) were deposited on DSPE-coated quartz surfaces by the Langmuir–Blodgett deposition. Structural transitions in PEO2000 from pancake to mushroom, and from mushroom to brush conformations were revealed from film balance experiments. Adsorption kinetics of proteins from 1% platelet-poor plasma (PPP) on the supported lipid bilayers were studied using intrinsic total internal reflection fluorescence. All the supported lipid bilayers exhibited over a magnitude reduction in adsorbed plasma proteins, compared with the quartz substrate. The increase of PEO2000-DSPE density in the mixed bilayers slightly increases the amount of adsorbed proteins on the bilayers. © 2000 Elsevier Science Ltd. All rights reserved.

Keywords: Protein adsorption; Polyethylene oxide conformation; Steric repulsion; Total internal reflection fluorescence

1. Introduction

Non-specific adsorption of plasma proteins on biomaterials is believed to initiate many adverse biological consequences, including blood coagulation, platelet adhesion and complement activation [1–3]. The adsorption of plasma proteins on liposomes, used as drug delivery carriers, is believed to be a major cause for their rapid clearance from the circulation by the reticular endothelial system. Grafting water-soluble polymers like poly (ethylene oxide) (PEO, also known as PEG) onto the surface of colloidal particles and biomaterials has been shown to improve biocompatibility [4,5]. In the case of sterically stabilized liposomes, grafting PEO on liposome significantly prolongs their circulation time in vivo [6], which is attributed to steric repulsion of plasma proteins by the grafted polymers [7]. However, relatively few studies have examined the mechanisms of non-specific protein adsorption on liposomes during the clearance

process. This can be attributed to the lack of sensitive in situ surface analytical methods for studying protein interactions with the microscopic liposomal vesicles, which have a typical diameter of ∼100 nm.

The conformation of the surface-grafted PEO chains, as a function of their density, was determined recently, using neutron reflectometry of supported planar phospholipid monolayers and bilayers [8]. Force profiles between two supported phospholipid bilayers grafted with PEO also have been measured using a surface force apparatus [9]. Steric repulsion forces were correlated with the grafting density of PEO. Supported lipid bilayers, with surface-grafted PEO, provide a close approximation of the outer surfaces of PEO–liposomes. The supported bilayers can be prepared on solid substrates, using the Langmuir–Blodgett (LB) deposition, to obtain well-defined compositions and structures. Compared with vesicles, supported bilayers allow direct structural and property analysis of the polymer-coated lipid surfaces, and in situ functional studies.

In this report, the adsorption of plasma proteins on PEO-grafted lipid bilayers was studied using the surface-sensitive total internal reflection fluorescence (TIRF) spectroscopy. TIRF spectroscopy has been used successfully to study adsorption kinetics of proteins on a variety

* Correspondence address: Department of Biomedical Engineering, Wickenden Building, Case Western Reserve University, Cleveland, OH 44106, USA. Tel.: 216-368-3005; fax: 216-368-4969.
E-mail address: rxm4@po.cwru.edu (R.E. Marchant).

of surfaces [10,11]. This highly sensitive fluorescence technique allows quantification of pg-ng/cm^2 amounts of adsorbed proteins in real time. The spectroscopic nature of TIRF also makes it potentially useful for studying other aspects of protein adsorption including adsorption kinetics, competitive adsorption kinetics, conformational changes in the adsorbing proteins, and the surface rotational and lateral mobility of adsorbed proteins [12,13].

In this study, supported lipid bilayers on quartz are prepared by LB deposition from mixtures of distearoylphophatidylcholine (DSPC) and PEO (molecular weight 2000)-grafted distearoylphosphatidylethanolamine (PEO2000-DSPE). Surface coverage of PEO on the outer layer was adjusted by changing the mole fraction of PEO–DSPE in the lipid mixture from 0 to 10%, and by changing the surface area occupied per molecule during LB deposition. Adsorption kinetics from 1% platelet-poor plasma (PPP) diluted with phosphate-buffered saline (PBS) on the bilayers was studied by intrinsic TIRF spectroscopy using the tryptophan residues in the adsorbed proteins. Since most plasma proteins contain at least one tryptophan residue, intrinsic TIRF provides a convenient approach to investigate non-specific adsorption of plasma proteins.

2. Experimental section

2.1. Chemicals and proteins

Distearoyl phosphatidylcholine (DSPC), distearoyl phosphatidylethanolamine (DSPE), and PEO2000-DSPE (Fig. 1) were purchased from Avanti Polar Lipids Inc. (Alabaster, AL) in powder form or in chloroform solution.

Water was pretreated with an exchange carbon tank, a water softener, and purified by a Milli-RO 120 unit. It was then fed through a Milli-Q PLUS unit, which treats the water with UV light (185 and 254 nm) followed by a 0.22 µm Millipak 40 filter. The resistance of the purified water is greater than 18.2 MΩ cm. Phosphate-buffered saline (PBS, Sigma), containing 10 mM phosphate salt, 120 mM NaCl, and 2.7 mM KCl at pH 7.4, was used as the buffer for protein solutions.

To obtain 1% Platelet-poor plasma in PBS (1% PPP) venous blood was collected from healthy aspirin-refraining donors. Whole blood was drawn into a sterile syringe, containing the filtered anticoagulant sodium citrate (Sigma), to a final blood : sodium citrate ratio of 9 : 1. PPP was obtained by centrifuging the blood sample at 1100 g for 25 min. PPP was aliquoted and stored at −70°C. 1% PPP was prepared by diluting PPP in PBS, and used within one day. All other proteins were obtained from Sigma. Protein concentrations were determined by the Bradford method [14] using a standard Coomassie protein assay (Pierce, Rockford, IL). Calibration of the TIRF instrumental sensitivity was performed using 5-hydroxy-L-tryptophan·HCl (TRP, Calbiochem) in PBS.

2.2. Deposition of bilayers

Quartz slides (BioElectro Spec Inc., Starkville, MS) were used as substrates for the bilayer deposition. The quartz slides were cleaned by an argon radiofrequency discharge in a Branson/IPC discharge chamber for 15 min. The slides were then immersed in a freshly prepared hot acid 'piranha' mixture (3 : 1 v/v concentrated H_2SO_4 and 30% H_2O_2) and subsequently rinsed with ethanol and water. The cleaned slides were kept under Millipore water and used for LB bilayer deposition within two days.

Langmuir–Blodgett (LB) deposition was used to construct supported planar bilayers on the quartz slides. The LB trough (KSV5000, KSV Instrument Ltd., Finland) consisted of two baths of dimensions of 12×70 cm^2. The
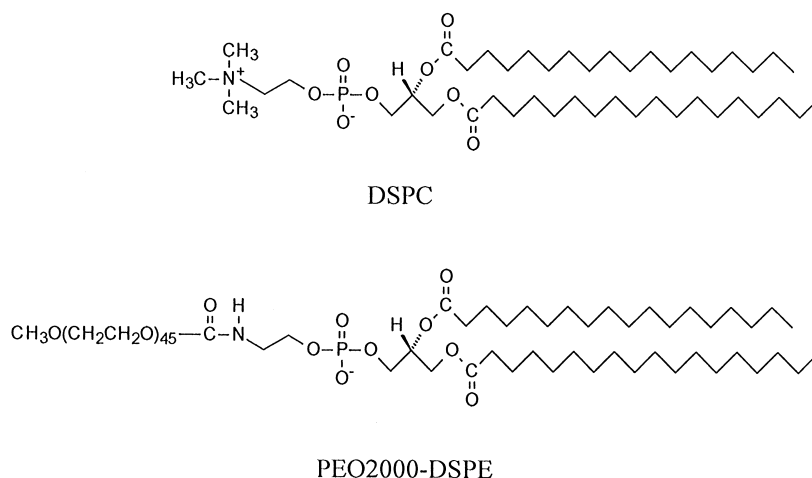

DSPC

PEO2000-DSPE

Fig. 1. Structure of the zwitterionic lipid DSPC and the polyethylene oxide-modified lipid PEO2000-DSPE.

trough was placed on an anti-vibration table in a class 100 clean room, to reduce mechanical distortion and contamination of the films. The trough was carefully cleaned with precision wipe paper dipped in chloroform, and rinsed with water. The subphase used was pure water, maintained at $21 \pm 1°C$. The surface of the liquid subphase was cleaned using a suction system. Phospholipid solutions (70–100 μl, 1 mg/ml in chloroform) were spread on the water subphase, and the chloroform was allowed to evaporate for 10 min. The monolayers were compressed symmetrically with two moving barriers at a speed of 24 cm²/min until a surface pressure of 40–45 mN/m was reached. At this pressure, the DSPC layer is in the solid gel phase with an area of approximately 0.44 nm² per molecule. Similar surface pressures were used for all concentrations of PEO2000-DSPE.

The characteristic surface pressure–area (π–A) isotherms, and creep test data measured by a platinum Wilhelmy plate attached to a balance, were collected to determine the optimum conditions for LB deposition. In the creep test, the film is compressed to the operating surface pressure. The monolayer is held at constant pressure, and the change in the area with time is recorded. A film was defined as stable, when the change in area was less than 6% over 1 h.

Once a film's stability was established, deposition of the first pure DSPE monolayer onto a quartz slide was performed by withdrawing the slide through the air/water interface at a rate of 2 mm/min, while the film pressure was held at 40 mN/m. It is believed that an interfacial potential created by the hydrophilic head of the zwitterionic phosphatidylcholine attracts the negatively charged quartz surface to provide physical attachment of this first layer onto the quartz. The second layer of DSPC, containing 0–10% PEO2000-DSPE, was constructed in a similar manner, except that the DSPE deposited slide was dipped through the air/water interface at 42–45 mN/m. The second layer is physically bound to the DSPE-coated quartz by hydrophobic interaction between the alkyl tails of the DSPC and DSPE monolayers. Since exposure of the bilayer coated surface to air could cause the removal of the outer monolayer, the quartz slide was kept under water after LB deposition. LB film transfer ratios were always close to unity for the first layer, and ~ 0.9 for the second layer. This may indicate the formation of a slightly mixed X–Y-type film, instead of an ideal Y-type film.

2.3. TIRF instrumentation

TIRF measurements were performed on a Fluorolog-3, Model 3-12, spectrofluorometer (Instruments S.A. Inc., Edison, NJ) assembled with a pre-aligned, surface-selective fluorescence TIRF flow cell (BioElectroSpec Inc., Starkville, MS). An illustration of the system is shown in Fig. 2. The spectrofluorometer uses a 450W xenon lamp
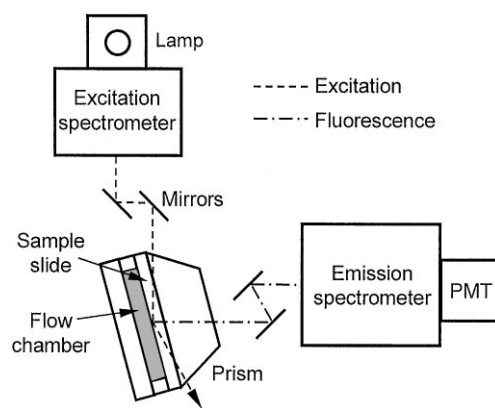

Fig. 2. Schematic structure of the TIRF setup. Incident angle of the excitation beam is fixed at 75°. Dimension of the flow chamber is $2 \times 1 \times 0.025$ cm².

as excitation source. The excitation, emission, polar and synchronous scans allow automatic acquisition of uncorrected and/or corrected excitation and emission spectra, polarization and synchronous luminescent spectra, while a time-based intensity scan monitors fluorescence as a function of time. The combination of a single-grating excitation spectrometer and a double-grating emission spectrometer provided optimum performance in resolution, sensitivity and stray-light rejection for highly scattering samples such as proteins, membranes and solid samples. The fluorescence intensity was measured in photon counting mode. The sensitivity of the spectrofluorometer was demonstrated by its detection of 50 femtomolar fluorescein in solution. In addition, when the spectrofluorometer is operated in TIRF mode, we have been able to detect the adsorption of fluorescein isothiocyanate (FITC)-labeled fibrinogen on octadecyltrichlorosilane (OTS)-modified quartz with a surface density as less as a few molecules per μm², as determined by atomic force microscopy.

The TIRF flow cell is a sandwich design (Fig. 2). The dovetail quartz prism was coupled with glycerol to the testing quartz slide. A polyurethane gasket and a quartz back block, with ports for solution injection, formed the TIRF flow field. The flow cell sandwich was fixed into a frame by an alumina cover, and mounted onto the alignment platform of the Florolog-3 sample insert assembly. The incident angle of the excitation light was fixed at 75°, exceeding the critical angle for total internal reflection at quartz/water interface ($\theta_{crit} = 64.7°$). The volume of the flow chamber ($1 \times 2 \times 0.025$ cm²) was approximately 50 μl. For this narrow TIRF flow compartment (thickness of the gasket, $b = 0.025$ cm), the corresponding wall shear rate, γ, given by Eq. (1), was attained in the flow chamber with width, $w = 1$ cm, at a typical volumetric flow rate, V, of 0.4 ml/min

$$\gamma = 6V/wb^2 = 64 \, \text{s}^{-1}. \tag{1}$$

The corresponding shear stress, τ, with PBS solution (viscosity, $\eta = 0.00684$ poise) was

$$\tau = \eta\gamma = 0.44 \text{ dyn/cm}^2. \tag{2}$$

2.4. Calibration of TIRF

TIRF utilizes the evanescent wave generated by the total internal reflection of a light beam at the interface between two transparent media when the incident angle is greater than the critical angle. The evanescent wave, which decays exponentially, interacts with optically less dense medium, such as a protein solution. Only fluorophores adjacent to the interface are excited. The evanescent wave provides surface sensitivity to TIRF and allows measurements of surface concentrations of adsorbed molecules in the presence of relatively high concentrations of the same molecules in the bulk solution.

Quantification of intrinsic TIRF is well documented [15]. Briefly, the physical properties of the evanescent wave are governed by Eqs. (3) and (4). The electric field amplitude for the evanescent wave, E, decays exponentially in solution from the interface (Fig. 3)

$$E = E_0 e^{-z/d_p}. \tag{3}$$

The characteristic penetration depth, d_p, defined as the distance from the interface, where the intensity of evanescent wave is reduced to e^{-1} of its original value, is dependent on wavelength, λ, the angle of incidence, θ, and refractive indices of the quartz (n_1) and aqueous solutions (n_2):

$$d_p = \frac{\lambda}{2\pi} (n_1^2 \sin^2 \theta - n_2^2)^{-1/2}. \tag{4}$$

For the experimental conditions used in this study, the penetration depth was calculated as 74 nm for $\lambda = 280$ nm, $n_1 = 1.515$, $n_2 = 1.333$, and $\theta = 75°$.

The observed fluorescence intensity (I) at chosen excitation and emission wavelengths is governed by the extinction coefficient, ε, the quantum yield, φ, the concentration of fluorophores, c, and the intensity of the evanescent wave, $(E)^2$. They are all dependent on the distance from the interface, yielding:

$$I = k \int_0^{d_{cell}} \varepsilon(z)\varphi(z)c(z)(E(z))^2 \, dz, \tag{5}$$

in which k is an instrumental factor dependent on the efficiency of detecting the fluorescence. Since the observed fluorescence intensity is governed by properties of the fluorophore as well as instrumental setup, it must be calibrated using standard fluorophore solutions for quantitative analysis. In this study, we used TRP solutions of relatively high concentration ($\varepsilon_c = 20$, 25, 30 cm^{-1}) as calibration standards. Under these concentrations, the scatter-originated signal was constant, while the evanescently excited signal increased linearly with the TRP concentration in solution (Fig. 4). This linear increase was used to normalize the observed fluorescence intensity. The relative quantum yields of different proteins were obtained by measuring the intrinsic fluorescence intensities of protein solutions by exchanging the TRIF assembly with the standard cuvet sample holder.

This calibration procedure provides a reliable means for comparing the adsorption of proteins on different surfaces. However, the absolute amount of protein adsorbed cannot be determined because the exact composition of the protein layer adsorbed is unknown. This procedure also includes some uncertainties when intrinsic
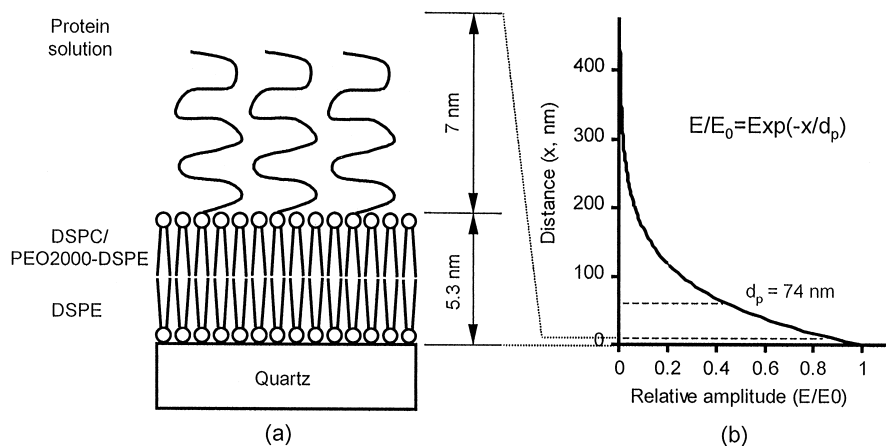

Fig. 3. (a) Schematic structure of the mixed DSPC and PEO2000-DSPE bilayer deposited on quartz surface. The top layer containing 10% of PEO2000-DSPE results in a brush conformation for the PEO molecules and a layer thickness of ∼7 nm; (b) the exponentially decaying electric field amplitude of evanescent wave above the bilayer. Penetration depth is calculated as 74 nm for the experimental conditions used in this study.

Enzymatic lipid removal from surfaces—lipid desorption by a pH-induced "electrostatic explosion"

Torben Snabe, Maria Teresa Neves-Petersen, Steffen Bjørn Petersen*

Department of Physics and Nanotechnology, Biostructure and Protein Engineering Group, Aalborg University, DK-9000 Aalborg, Denmark

Abstract

Removal of lipidic molecules from surfaces can be accomplished using detergents containing lipases. Surface cleaning is usually performed under alkaline conditions due to increased solubility of the hydrolysis products, especially free fatty acids. This paper shows that removal of a triacylglycerol film from a surface can be dramatically enhanced in a sequential system where pH is shifted to alkaline conditions after an initial lipolytic reaction period at or below neutral pH. Data from three different biophysical techniques, attenuated total reflection Fourier transform infrared spectroscopy (ATR-FTIR), quartz crystal microbalance with dissipation monitoring (QCM-D), and total internal reflection fluorescence spectroscopy (TIRF) clearly show the effects of such cleaning procedure. Initially the reaction is carried out at pH below the pK_a value of the fatty acids formed upon triacylglycerol hydrolysis, and the protonated fatty acids accumulate in the film. The mechanism of lipid removal, induced by increasing pH to a value above the fatty acid pK_a, is explained by a burst caused by electrostatic repulsion between rapidly ionised fatty acids, i.e. by an "electrostatic explosion". Performing the initial hydrolysis at pH 6 and the subsequent rinse at pH 10, using triolein as model substrate, lipid removal from surfaces by both commercial detergent lipases and non-commercial lipases was significantly improved compared to a reaction at constant pH 10.
© 2004 Elsevier Ireland Ltd. All rights reserved.

Keywords: Lipase activity; Lipid removal; Lipase adsorption; Triacylglycerol; ATR-FTIR; QCM-D; TIRF

1. Introduction

A major problem when cleaning surfaces is the removal of adsorbed lipid deposits, which often contain oily, longchained, and water-insoluble triacylglycerols. Detergent formulations usually contain lipolytic enzymes (lipases, formally triacylglycerol lipases, E.C. 3.1.1.3), which degrade triacylglycerols into free fatty acids, di- and mono-acylglycerols, and possibly glycerol. These hydrolysis components, especially the fatty acids, are more water soluble compared to triacylglycerols (Fujii et al., 1986). With aid from

detergent components and their ability to form water soluble aggregates, fatty acids may solubilize into the aqueous washing solution and thereby be released from the surface. Lipases are essential in detergent formulations when cleaning at low temperatures (Dambmann et al., 1971).

The lipase from *Thermomyces lanuginosus*, formerly *Humicola lanuginosa*, was the first major commercial lipase for detergents. The *T. lanuginosus* lipase (TLL) is produced and sold by Novo (now Novozymes, Denmark) since 1989 as lipolase (Aaslyng et al., 1991). Though lipolase is stable in detergent formulations, at high pH, and at high temperatures, 2–3 wash cycles (which includes drying of the textile) are needed to obtain a significant removal of lipidic stains (Flipsen et al., 1998; Aaslyng et al., 1991).

One suggestion explaining this lack of "first wash activity" by lipolase is that the main lipolytic activity occurs during the drying process (Flipsen et al., 1998; Aaslyng et al., 1991). Triacylglycerol removal is therefore only achieved after the second wash when the detergent solution and the mechanical stress can remove the hydrolysis products produced during the first drying (Aaslyng et al., 1991).

We have outlined in a previous paper an alternative explanation, suggesting that the formation rate of ionised fatty acids (as a result of lipase activity) must exceed a certain threshold in order to obtain lipid removal (Snabe and Petersen, 2003). The mechanism is explained by an equilibrium between hydrolysis products being incorporated into the substrate film or forming micelle-like aggregates which can be solubilized and ejected into the aqueous solution. Interestingly, it was found that the equilibrium favours lipid removal only under alkaline and Ca^{2+}-free conditions and when the lipolytic rate is above a certain threshold. Consequently it was proposed that the equilibrium of lipid removal is controlled by the formation rate of ionised fatty acids.

Flipsen et al. (1998) reported an empirical study of the removal of triolein soil from textile using lipases. It was found that the triacylglycerol lipase cutinase displayed significant lipid removal (20%) at constant pH 9—thus cutinase can be termed a "first-wash lipase". However, in a sequential system where the initial incubation at pH 9 was followed by a subsequent wash at pH 10.5–11, the removal of lipid increased to 35%. The improvement was explained in terms of increasing

lipid solubility in aqueous environment at increasing pH values.

The present paper shows that significant lipid removal from surfaces by a large range of lipases can be induced by carrying out the washing procedure at two different pH values. The washing process is preferably started below the pK_a value of the released fatty acids. Hydrolysis should then be allowed to progress for some time allowing accumulation of protonated fatty acids in the lipid film. Subsequently the pH of the solution in contact with the surface to be cleaned is raised above the pK_a value of the fatty acid molecules. This procedure results in a significantly improved lipid removal (up to 50%) compared to the usual procedure performed under constant alkaline conditions. Using the longchained triolein as substrate, results are presented with the native *T. lanuginosus* lipase (TLL) and engineered TLL variants, as well as lipases from *Rhizomucor miehei*, *Pseudomonas cepacia*, and *Fusarium solani* pisi (cutinase).

2. Materials and methods

2.1. Materials

Triolein 99% (Fluka 92859, lot. 2045347) was used as substrate. Seven triacylglycerol lipases (E.C.3.1.1.3) were used: *T. lanuginosa* lipase (TLL) and engineered TLL variants, i.e. lipolase, lipoprime, lipex, and an inactive TLL (Novozymes, Denmark), as well as lipases from *R. miehei* (Sigma L9031, lot 32K2604) *Ps. cepacia* (Sigma L9156, lot 85H2604), and *F. solani* pisi (cutinase) produced in our laboratory (Petersen et al., 1998). Protein concentrations were determined using UV_{280} absorption and the respective extinction coefficients at 280 nm. Buffer of 3×25 mM citrate–Tris–glycine (25 mM of each component) with or without 10 mM $CaCl_2$ was prepared from citrate trisodium dihydrate 99% (Sigma S4641,19H0717), glycine 99.5% (Acros Organics, 220910010/200-272-2), Tris 99.9% (Applichem A1086,C2101), and calcium chloride dihydrate 99.5% (Merck 1.02382, lot TA401282). pH was adjusted with 3 M sodium hydroxide or hydrochloric acid and filtered through a 0.20 μm filter before use (Sartorius Minisart 16534 K). Reagents for preparation and triolein coating of TIRF quartz slide surfaces: dichlorodimethylsilane (Fluka 40150,

lot 413248/1), trichloroethylene (Aldrich 13,312-4, lot U00885), 1% (v/v) triolein in *n*-hexane (Merck 1.04367 lot I1020367-142). Reagents for preparation of gold QCM-D crystal surfaces: octadecylmercaptan 98% (Sigma O185-8, lot 17625-0201) in *n*-hexane. For oleic acid film titration, oleic acid (Sigma O1630, lot 48H5218) was used.

2.2. Methods

Lipolysis of a triolein film on a hard surface support was analyzed. ATR-FTIR and QCM-D was used for chemical and physical analysis of the lipid film, while TIRF was used for monitoring lipase adsorption to the film. All experiments were performed at 25 °C (±0.5 °C).

2.2.1. ATR-FTIR analysis of the remaining film after hydrolysis

Chemical analysis of the remaining lipid film after the lipolytic reaction was performed using attenuated total reflection infrared spectroscopy (ATR-FTIR).

2.2.1.1. ATR-FTIR Instrumental. A Bruker IFS 66V/S FTIR spectrometer with a deuterium triglycine sulphate (DTGS) detector was used (purchased from Bruker Optics, Germany). The sampling unit was a 1 cm × 7 cm large 45° ZnSe attenuated total reflectance (ATR) crystal with six internal reflections at the crystal–sample interface. The ATR crystal made out the base in a reaction chamber of height ∼0.1 cm and a total volume of ∼1.1 ml (Fig. 1). A continuous flow through
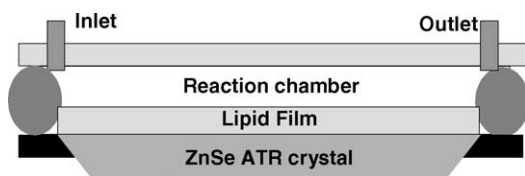

Fig. 1. Set-up of the ATR-FTIR flow reaction chamber, with the ZnSe ATR crystal as base, a rubber O-ring as spacer wall, and a plexiglass plate as lid. The incident infrared radiation angle was 45° and six internal reflections were introduced to the active surface (towards the reaction chamber). The volume of the reaction chamber was approximately 1.1 ml, created by a height of 0.1 cm and a total base area of 11 cm^2 (of which 7 cm^2 was the ATR crystal and the remainder was the surrounding teflon-coated crystal holder). Note that dimensions are not in correct proportions.

the chamber was applied using a peristaltic pump. Each spectrum was averaged from 32 scans recorded at a scan rate of 10 kHz at a resolution of 4 cm^{-1}. Data was collected in the 4000–800 cm^{-1} range. The general theory and applications of the ATR-FTIR technique have been covered in sufficient depth elsewhere (Harrick, 1967; Griffiths and de Haseth, 1986) and is therefore not described further in the present paper. Specifically for triacylglycerol film analysis we refer to Snabe and Petersen (2002, 2003).

2.2.1.2. ATR-FTIR experimental. Experiments were performed using the following procedure: A thin film of pure triolein was carefully applied by distributing a drop uniformly on the hydrophobic ZnSe ATR crystal surface with a cotton stick until the absorbance for the carbonyl ester peak (1745 cm^{-1}) was 0.28–0.32 absorbance units. After mounting the lid, the water insoluble triolein film was exposed to buffer at pH 6 or 10 for 10 min (a volume of 5 ml buffer circulated through the reaction chamber using a peristaltic pump at a constant flow rate of 3.5 ml min^{-1}). Then hydrolysis was initiated by circulating a fresh buffer solution at pH 6 or 10 with lipase through the reaction chamber for 20 min. After 20 min, fresh "rinsing buffer" at pH 10 was circulated in the system for 10 min. Subsequently, the reaction chamber was drained before the film was exposed to a buffer at pH 10 with 10 mM Ca^{2+} for 2 min. Finally, the chamber was drained again and the film was allowed to air dry before an infrared spectrum of the remaining lipid film was recorded.

The relative content of total lipid remains on the ATR crystal were analyzed by simple absorption spectrum integration of the hydrocarbon region at 3050–2700 cm^{-1} (mainly CH$_2$ and CH$_3$–vibrations). The presence of fatty acid products in the film were identified in the region at 1600–1520 cm^{-1} (fatty acid carbonyl vibrations in complex with Ca^{2+}). Lipids in the reaction buffer (at pH 6 or 10) and the rinsing buffer (at pH 10) were extracted by mixing thoroughly with 25% *n*-hexane. The extracted lipids were analyzed qualitatively by applying 10–20 μl of the hexane phase on the ATR crystal surface. After evaporation of the hexane an infrared spectrum of the extracted lipids was recorded. After each measurement, the ATR crystal surface was cleaned carefully using ethanol and lens paper.

2.2.2. ATR-FTIR analysis of oleic acid ionisation

In order to observe the ionisation state of oleic acid as a function of pH, a thin film of pure oleic acid was applied on the ATR crystal and exposed to buffers ranging from pH 5–10. After 5–10 min of incubation with buffer the sample spectrum (oleic acid with buffer) was recorded using the pure buffer spectrum as background. The resulting spectra were normalised against the CH$_2$–peak at $\sim$1465 cm^{-1} in order to improve the visualisation.

2.2.3. QCM-D analysis of the lipid film during hydrolysis

Quartz crystal microbalance with dissipation monitoring (QCM-D) was applied for lipid film characterisation (film thickness and viscoelastic properties) during lipolytic degradation.

2.2.3.1. QCM-D instrumental.
QCM-D is a state-of-the-art technique for surface analysis in liquid media. The technique is based on the oscillation of a piezoelectric quartz crystal dish where the oscillation frequency (F) and the oscillation energy dissipation (D) characterises the mass and the viscoelastic properties of the molecules adsorbed on the crystal surface. Adsorption of biomolecules to surfaces and viscoelastic characterisation of polymer films are among the usual applications. The technique for the current purpose—characterisation of a triolein film during enzymatic degradation—has recently been described in detail (Snabe and Petersen, 2003). Among other relevant references to the QCM-D technique the authors refer to Rodahl et al. (1997), Höök et al. (1999, 2001), Voinova et al. (1999).

A quartz crystal microbalance and dissipation device (Q-Sense D301) purchased from Q-Sense AB (Göteborg, Sweden) and a gold-coated piezoelectric quartz crystal with a fundamental frequency of 5 MHz was used. The active gold surface of the 14 mm large quartz crystal (diameter) formed the base in a reaction chamber with a volume of $\sim$80 µl (height $\sim$0.5 mm) in which a rapid exchange of reaction liquid was possible (Fig. 2).

2.2.3.2. Surface preparation and triolein film coating of the QCM-D crystal surface.
The gold surface on the QCM-crystal is hydrophilic. In order to achieve a hydrophobic surface, a monomolecular alkane
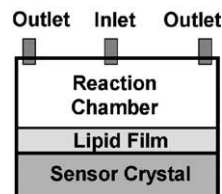

Fig. 2. The QCM-D set-up with the piezoelectric quartz crystal sensor as base in the reaction chamber. The sensor surface is circular with a diameter of 14 mm and the chamber height is $\sim$0.5 mm, i.e. the chamber volume is $\sim$80 µl. Note that dimensions are not in correct proportions in this illustration.

(octadecyl) film with a terminal thiol group (–SH) was covalently bound to the gold surface. Before preparing the surface, a thorough cleaning process was conducted, where the crystal first was illuminated with UV-light for 30 min, then immersed into a solution of 1:1:5 of H$_2$O$_2$:NH$_3$:deionised H$_2$O at 75 °C for 5 min, and subsequently rinsed thoroughly with deionised water. The crystal was then immersed into a solution of 1 mM octadecylmercaptan (HS(CH$_2$)$_{17}$CH$_3$) in *n*-hexane for at least 2 h at ambient room temperature (20–25 °C), rinsed in pure *n*-hexane, ethanol, and deionised water, and finally dried with nitrogen gas.

2.2.3.3. QCM-D experimental.
A triolein film was prepared manually by carefully distributing a drop of pure triolein on the hydrophobic QCM-D quartz crystal surface using a piece of soft lens paper. The shift of the fundamental frequency was within 250–500 Hz. Before applying the enzyme, the film was hydrated in the buffer (pH 6 or 10) for 8 min upon adding fresh buffer three times. Every buffer addition was performed by entering 0.5 ml through the reaction chamber, ensuring thorough exchange of the liquid in the reaction chamber (flow was controlled by gravity—buffer exchange lasted 3–5 s). Enzyme addition was performed also by letting 0.5 ml lipase solution (2 µg ml^{-1}) in the same buffer stream through the measurement chamber. After 20 min hydrolysis, 0.5 ml buffer at pH 10 was applied.

The frequency (F) and dissipation (D) were obtained for the fundamental frequency, the 3rd, and the 5th overtone (i.e. 5, 15, and 25 MHz) and modeled using the viscoelastic model based on the Voight representation (software: Q-Tools, Q-Sense AB, Göteborg). The viscoelastic model is applicable for polymeric films with predominantly liquid characteristics and provides

modeled values of the film thickness (d_f), viscosity (η_f), and elasticity (μ_f). Model details are described elsewhere (Voinova et al., 1999; Höök et al., 2001; Snabe and Petersen, 2003). Model constants were the solvent density ($\rho_l = 10^3 \, kg \, m^{-3}$), the solvent viscosity ($\eta_l = 10^{-3} \, kg \, m^{-1} \, s^{-1}$), and the film density ($\rho_f = 0.95 \cdot 10^3 \, kg \, m^{-3}$). Initial values for the variable film parameters were: $\eta_f = 4 \, kg \, m^{-1} \, s^{-1}$; $\mu_f = 1.5 \times 10^5 \, Pa$; $d_f = 100 \, nm$.

After each measurement, the system was cleaned with helmanex (non-ionic detergent), 99% ethanol, and deionised water, and subsequently dried with nitrogen gas. A sufficient surface hydrophobicity was verified by visually controlling that the contact angle of a water drop on the crystal surface was more than $90°$.

2.2.4. TIRF measurements

Total internal reflection fluorescence (TIRF) spectroscopy was used in order to monitor lipase adsorption and desorption from a hydrophobic surface coated with triolein.

2.2.4.1. TIRF instrumental. TIRF employs the phenomenon of total internal reflection of an electromagnetic wave that occurs at the interface between two transparent media with different refractive indices when the incident angle is greater than the critical angle. In brief, when a beam of light propagating within a medium of higher refractive index (n_1) (e.g. quartz) encounters an interface with a medium of lower refractive index (n_2) (e.g. water) the light undergoes total internal reflection if the incident angles (θ_i) is greater than the critical angle (θ_c). The critical angle is defined as $\theta_c = \sin^{-1}(n_1/n_2)$. Interference of the incident and reflected beams generates a standing electromagnetic wave with maximum amplitude of the electric vector at the interface. An exponentially decaying electromagnetic wave, the evanescent wave, penetrates into the less condensed medium (i.e. the aqueous solution), while the main part of the incident light is reflected back into optically more condensed medium of quartz. The penetration depth (d_p) of the evanescent wave into the sample medium is a function of the incidence angle, the refractive index ratio, and the incident light wavelength (λ_i):

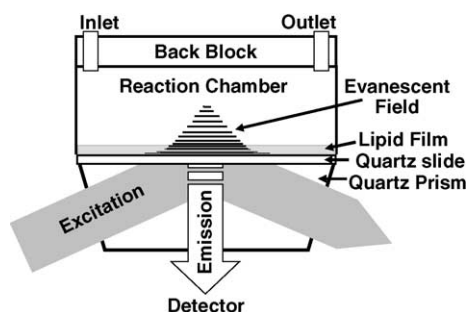$$d_p = \lambda_i [(2\pi n_1)(\sin^2(\theta_i) - (n_2/n_1)^2)^{0.5}]^{-1}.$$

Fig. 3. Illustration of the TIRF flow cell. The volume of the reaction chamber is approximately 3.5 μl, created by a height of 0.01 mm and a base area of approximately 350 mm² (a rectangular shape of 16 mm broad and 24 mm long with cut edges). Note that dimensions are not in correct proportions.

In the current system the penetration depth of the evanescent field is in the order of 112 nm ($\theta_i \approx 72°$; $\lambda_i = 280 \, nm$; $n_{quartz} = 1.46$ and $n_{water} = 1.33$). Thus, the evanescent wave provides surface selectivity to TIRF and allows measurements of surface concentration of fluorescent adsorbed molecules, e.g. proteins.

A TIRF system (BioElectroSpec Inc., Harrisburg, PA) coupled with a fluorescence spectrophotometer (PTI QM-2000 from Photon Technology Int., Lawrenceville, NJ) with a 75 W Xenon arc source was used. The PTI instrument excitation and emission slits were set to 6 nm. The sample in the flow chamber was excited at 280 nm and the fluorescence emission intensity was monitored at 330 nm. The flow chamber was comprised by a "sandwich" consisting of a TIRF quartz prism, a TIRF quartz slide (with the sample surface), a 10-μm gasket (comprising the chamber thickness), and a back block with holes to channel the solution through the flow chamber (Fig. 3). The dimension of the flow chamber is 16 mm × 24 mm × 0.01 mm (3.8 μl). The excitation light travels through the prism and slide, hits the interface between slide and solution, and totally internally reflects from the interface back into the slide and prism. The reflected beam generates an evanescent electromagnetic field in the middle of the TIRF slide. This area of the TIRF slide serves thus as the sensor surface. Only fluorophores that are present at the surface and in close proximity of the surface (within the evanescent field) are excited and fluoresce.

2.2.4.2. Surface preparation and triolein film coating of the TIRF quartz slide. Chemical modification of

glass, quartz and metal oxide surfaces involves silanization. Silane chemistry allows functionalisation of a quartz surface with different active groups, such as methyl groups. In order to prepare a hydrophobic surface for TIRF measurements (in order to improve lipid adhesion), the quartz slide was methylated by incubating the surface with 0.3% (v/v) dichlorodimethylsilane in trichloroethylene for 30 min at ambient room temperature (20–25 °C). Subsequently, the surface was rinsed in pure trichloroethylene for 5 min and finally flushed thoroughly with ethanol and deionised water before drying with nitrogen gas. The methylation procedure was based on a procedure described by Buijs and Hlady (1997). The methylated slide was then attached on the TIRF quartz prism using glycerol in between them (glycerol and quartz have almost equal refractive indices and let the light pass with minimal interference). The triolein film was prepared by distributing 20 μl triolein–hexane solution (0.1%, v/v) on the methylated surface using the side of a pipette tip. After hexane evaporation, the triolein film appeared as a homogeneous "foggy" film on the surface.

2.2.4.3. TIRF experimental. The TIRF flow-chamber was prepared by placing the gasket between the triolein coated slide/prism and the back block and mounted vertically in the instrument. Buffer with and without lipase was purged through the chamber at a flow rate of 0.25 ml min^{-1}. Experiments were performed by an initial hydration in buffer without lipase for approximately 5 min before adding 2 μg ml^{-1} lipase in the same buffer (at pH 6 or 10). After 10–15 min the system was rinsed in buffer without lipase at pH 10. Fluorescence emission intensity at 330 nm (from excitation of aromatic protein residues at 280 nm) was monitored continuously during experiments (one measurement per second). After each experiment the surface was cleaned carefully with ethanol and deionised water and dried with nitrogen gas. The same surface was usable 20–30 times. A sufficient surface hydrophobicity was verified visually by controlling that the contact angle of a water drop on the crystal surface was more than 90°.

3. Results

The hydrolysis of a triacylglycerol film was monitored in two different pH systems. In the first system

the reaction was performed under constant alkaline conditions at pH 10 (called the pH 10 system), and in the second system the reaction was carried out at pH 6 followed by a rinse at pH 10 (called the pH 6–10 system).

3.1. Chemical film analysis (ATR-FTIR)

Based on integration of the hydrocarbon peaks at 3050–2700 cm^{-1} in the infrared spectra of the remaining dry film after the reactions, the relative levels of total lipid (both hydrolysed and non-hydrolysed) were computed (Fig. 4). It is observed that removal of lipid molecules is enhanced in the pH 6–10 system compared to the pH 10 system. This is true for all the lipases tested—except for lipoprime where the level of the remaining lipid film is equally low in both systems. Lipolase was tested at two concentrations (2 and 10 μg ml^{-1}). In the pH 6–10 system a concentration effect on lipid removal was observed, i.e. using 10 μg ml^{-1} lipolase results in the largest lipid removal, while no concentration effect was found in the pH 10 system. The control experiments without protein show an equal high level of remaining lipid in the pH 10 and 6–10 system.

In addition, for all lipases it was observed visually that lipidic bodies were released immediately from the surface when pH was shifted to pH 10 after the initial reaction at pH 6 (observed by looking into the reaction chamber through the transparent chamber lid when pH was shifted).

A qualitative activity control was carried out by detecting if free fatty acids had been formed and were present on the film after the reaction. When no lipase was added, no fatty acids were detected in either pH system, while for all lipases tested fatty acids were detected in both pH-systems, showing that lipolytic activity had occurred (data not shown).

Analysis of the supernatant in the pH 10 system showed that only fatty acids and no ester molecules were released into the aqueous phase (in this reaction ester containing molecules can be monoolein, diolein, and triolein). It is important to note that in the pH 6–10 system both fatty acids and ester molecules were released into the aqueous solution when shifting from pH 6 to 10 (data not shown).

Adsorption of Poly(ethylene glycol)-Modified Lysozyme to Silica

Susan M. Daly, Todd M. Przybycien, and Robert D. Tilton*

Departments of Chemical Engineering and Biomedical Engineering, Center for Complex Fluids Engineering, Carnegie Mellon University, Pittsburgh, Pennsylvania 15213

Covalent grafting of poly(ethylene glycol) (PEG) to pharmaceutical proteins, "PEGylation", is becoming more commonplace due to improved therapeutic efficacy. As these conjugates encounter interfaces in manufacture, purification, and end use and adsorption to these interfaces may alter achievable production yields and in vivo efficacies, it is important to understand how PEGylation affects protein adsorption mechanisms. To this end, we have studied the adsorption of unmodified and PEGylated chicken egg lysozyme to silica, using optical reflectometry, total internal reflection fluorescence (TIRF) spectroscopy, and atomic force microscopy (AFM) under varying conditions of ionic strength and extent of PEG modification. PEGylation of lysozyme changes the shape of the adsorption isotherm and alters the preferred orientation of lysozyme on the surface. There is an abrupt transition in the isotherm from low to high surface excess concentrations that correlates with a change in orientation of mono-PEGylated conjugates lying with the long axis parallel to the silica surface to an orientation with the long axis oriented perpendicular to the surface. No sharp transition is observed in the adsorption isotherm for di-PEGylated lysozyme within the range of concentrations examined. The net effect of PEGylation is to decrease the number of protein molecules per unit area relative to the adsorption of unmodified lysozyme, even under conditions where the surface is densely packed with conjugates. This is due to the area sterically excluded by the PEG grafts. The other major effect of PEGylation is to make conjugate adsorption significantly less irreversible than unmodified lysozyme adsorption.

Introduction

Covalent attachment of poly(ethylene glycol) (PEG) chains to therapeutic proteins, "PEGylation", is growing in application due to increased renal clearance time, decreased proteolytic degradation, and decreased immune response relative to the unmodified forms.[1,2] The PEGylated forms of adenosine deaminase and asparaginase are now approved for human use by the U.S. Food and Drug Administration,[2,3] and other PEG-modified proteins are being developed for possible therapeutic use, including PEG epidermal growth factor[4] and PEGylated single-chain Fv proteins.[5]

The numerous scenarios in which PEGylated proteins encounter solid/liquid interfaces during their manufacture, storage, and end use motivate this study of the effect of PEGylation on protein adsorption behavior. When PEGylated proteins are prepared for therapeutic applications, it is necessary that the distribution of modified forms be reproducible. Over-PEGylation can decrease bioactivity, and under-PEGylation may allow a molecule to be cleared from the circulatory system too rapidly. A reproducible population of modified forms could be achieved by controlling the PEGylation reaction and/or by fractionation of the PEGylated product. Chromatography is a common technique for therapeutic protein fractionation, and most chromatographic methods depend on adsorption behavior.

Furthermore, PEG-modified proteins may also encounter solid/liquid interfaces during drug delivery. Protein loss to deposition and surface-induced conformational changes at these interfaces is manifested as lost bioavailability. Tzannis and co-workers observed ∼90% loss of the biological activity of interleukin 2 after 24 h of continuous delivery via commercial silicone rubber catheter tubing.[6] Additionally, insulin activity is reduced upon delivery from micropumps, due to surface-induced aggregation.[7] In delivery technologies, where dosage is critical, unpredictable protein−surface interactions can have a significant impact on the amount of biofunctional drug administered to a patient. The extent of adsorption, the adsorption kinetics, and the layer structural evolution upon the adsorption of protein will dictate the yield of biochemically functional protein and will all likely be affected by PEGylation.

Interest in the adsorption of PEGylated proteins is piqued by the so-called "stealthy" characteristics of PEG. It is well-known that surfaces coated with PEG tend to be resistant to protein adsorption[8−10] and the protective effect of PEG modification on circulating proteins (as well as PEGylated liposomes) in vivo is attributed to strong steric and hydration repulsions between the PEGylated species and other proteins or cell surfaces.[11] Nevertheless, PEG itself is surface active on a variety of surfaces, and

* Corresponding author. E-mail: tilton@andrew.cmu.edu.

(1) Harris, J. M.; Martin, N. E.; Modi, M. *Clin. Pharmacokinet.* **2001**, *40*, 539.

(2) Michaelis, M.; Cinatl, J.; Pouckova, P.; Langer, K.; Kreuter, J.; Matousek, J. *Anti-Cancer Drugs* **2002**, *13*, 149.

(3) Hershfield, M. S. *Biochemistry and Immunology of Poly(ethylene glycol)-Modified Adenosine Deaminase (PEG-ADA)*; ACS Books: Washington, DC, 1997.

(4) Lee, H.; Park, T. *Pharm. Res.* **2002**, *19*, 845.

(5) Lee, L.; Conover, C.; Shi, C.; Whitlow, M.; Filpula, D. *Bioconjugate Chem.* **1999**, *10*, 973.

(6) Tzannis, S. T.; Hrushesky, W. J. M.; Wood, P. A.; Przybycien, T. M. *Proc. Natl. Acad. Sci. U.S.A.* **1996**, *93*, 5460.

(7) Sluzky, V.; Klibanov, A. M.; Langer, R. *Biotechnol. Bioeng.* **1992**, *40*, 895.

(8) Bergstrom, K.; Holmberg, K.; Safranj, A.; Hoffman, A. S.; Edgell, M. J.; Kozlowski, A.; Hovanes, B. A.; Harris, J. M. *J. Biomed. Mater. Res.* **1992**, *26*, 779.

(9) Gref, R.; Domb, A.; Quellec, P.; Blunk, T.; Mueller, R. H.; Verbavatz, J. M.; Langer, R. *Adv. Drug Delivery Rev.* **1995**, *16*, 215.

(10) Cheng, Y. L.; Darst, S. A.; Robertson, C. R. *J. Colloid Interface Sci.* **1987**, *118*, 212.

(11) Greenwald, R. B.; Choe, Y. H.; McGuire, J.; Conover, C. D. *Adv. Drug Delivery Rev.* **2003**, *55*, 217.

PEG modification of protein may not necessarily preclude or even decrease the extent of protein adsorption at the solid/liquid interface. Acid−base interactions between PEG ether groups and acidic groups on solid surfaces, such as the silanol groups on silica, make PEG surface active on many hydrophilic materials.[12,13] In addition, the somewhat hydrophobic character of PEG that causes it to have a lower critical solution temperature also makes PEG surface active on hydrophobic surfaces.[14] It is conceivable that the grafted PEG chain may have an adsorption affinity that is comparable to, or even stronger than, that of the protein. The variety of different possible driving forces for the adsorption of what amounts to a complex block copolymer, containing a protein "block" and one or more PEG blocks, makes for a complex adsorption energy landscape that is likely sensitive to the surface coverage and orientation of the PEG−protein conjugate.

Herein, we examine how the presence of PEG covalently grafted to a model protein, chicken egg lysozyme, affects the extent and reversibility of adsorption at the silica/water interface. We contrast the effects of covalently grafted PEG with the simple competitive adsorption of unmodified protein and PEG homopolymers. Chicken egg lysozyme is a commonly examined, relatively hard model protein with a low adiabatic compressibility that tends to resist surface-induced conformational changes on hydrophilic surfaces.[15,16] In addition to being a commonly used model substrate for protein adsorption studies, silica in various degrees of modification is also used as a chromatographic medium. We prepared our conjugates using 20 kDa PEG. Although early PEGylation strategies employed small PEG chains, on the order of a 5 kDa molecular weight or less, recent therapeutic applications focus on larger PEGs, including molecular weights of 20 and 40 kDa.[11] Increasing the molecular weight of the PEG moiety decreases the in vivo clearance rate of the conjugate.[17]

We recently reported experimental evidence that a two-stage, crowding-induced reorientation of unmodified lysozyme occurs during adsorption to the silica/water interface.[16,18] Consistent with a previously published model of electrostatic interactions within a lysozyme monolayer,[19] the reorientation optimizes both the lysozyme attraction to the oppositely charged silica surface and the lateral electrostatic repulsions among adsorbed protein molecules. The preferred orientation puts the active site toward the solution and the most positively charged amino acid patch (containing the N-terminus[20]) into contact with the negatively charged silica surface. This occurs when the adsorbed layer reaches a threshold surface coverage. The richness of this adsorption mechanism arises from spatially nonuniform intermolecular and surface forces. PEGylation imparts a new level of nonuniformity to the intermolecular forces and should be expected to significantly alter the adsorption mechanism.

Here, we report that PEG modification alters lysozyme adsorption isotherms, as well as the organization of the adsorbed layer at the silica/water interface. The complexity

of this adsorption problem dictates the use of multiple independent experimental tools. We use optical reflectometry[21−25] to monitor the extent and kinetics of adsorption and desorption, atomic force microscopy (AFM) force measurements[22,26−28] to characterize the extension of adsorbed conjugates at different surface coverages, and total internal reflection fluorescence[29−33] (TIRF) to monitor the exchangeability of unmodified and PEG-modified proteins or PEG homopolymer. We combine these conventional TIRF exchange experiments with the pH-sensitive fluorophore TIRF approach[18] to monitor reorientation dynamics that may occur within the PEG-modified lysozyme layer.

Experimental Section

Materials. Chicken egg lysozyme (Sigma, cat no. L-6876, lot no. 65H7025); methoxy-poly(ethylene glycol)-propionaldehyde (mPEG-propionaldehyde), nominal molecular weight 20 kDa (Nektar Therapeutics, formerly Shearwater Corporation); and poly(ethylene glycol) homopolymer, nominal molecular weight 20 kDa (Sigma-Aldrich Company), were used without further purification. All adsorption experiments were conducted in triethanolamine hydrochloride (TEA; Sigma-Aldrich Company) buffers prepared with varying ionic strength. The matrix assisted laser desorption/ionization (MALDI) matrix used with undigested proteins was 3,5-dimethoxy-4-hydroxycinnamic acid (Fluka). For protein digestion, we used iodoacetate (Sigma-Aldrich Company), dithiothreitol (DTT; Sigma-Aldrich Company), sequencing-grade-modified porcine trypsin (Promega Corporation), and α-cyano-4-hydroxycinnamic acid (Fluka). Fluorescein isothiocyanate (FITC) was obtained from Molecular Probes. Size exclusion chromatography was conducted in phosphate buffer made with sodium phosphate monobasic and dibasic salts (Fisher Scientific) and potassium chloride (Sigma-Aldrich Company).

Adsorption Substrates. Optical reflectometry and TIRF experiments were conducted on surface-oxidized optical-grade silicon wafers (Virginia Semiconductor) and quartz substrates (Bioelectrospec), respectively. We cleaned all surfaces by a protocol that is described in detail elsewhere.[16]

The substrates for the in situ AFM force measurements consisted of fused silica slides (Esco Products) and ultrasharp contact silicon cantilevers (K-Tek) with a 10 nm tip radius of curvature. A cantilever with a spring constant of 0.08 N/m was used for all experiments. The cantilever and the silica slide were cleaned by exposure to an ozone-generating UV lamp (Jelight Company, Inc.) for 30 min. After assembly of the AFM fluid flow cell, a 10 mM NaOH solution was injected. The silica slide and tip were soaked in this solution for 20 min followed by a profuse water rinse. This base treatment step was included to match the last cleaning step of the TIRF and optical reflectometry substrates.

PEGylation of Chicken Egg Lysozyme. We reacted chicken egg lysozyme with mPEG-propionaldehyde (1:6 mole ratio) in

(12) van der Beek, G. P.; Cohen Stuart, M. A.; Fleer, G. J.; Hofman, J. E. *Macromolecules* **1991**, *24*, 6600.
(13) Huang, Y.; Santore, M. M. *Langmuir* **2002**, *18*, 2158.
(14) Pagac, E. S.; Prieve, D. C.; Solomentsev, Y.; Tilton, R. D. *Langmuir* **1997**, *13*, 2993.
(15) Arai, T.; Norde, W. *Colloids Surf.* **1990**, *51*, 1.
(16) Daly, S. M.; Przybycien, T. M.; Tilton, R. D. *Langmuir* **2003**, *19*, 3848.
(17) Eliason, J. *BioDrugs* **2001**, *15*, 705.
(18) Robeson, J. L.; Tilton, R. D. *Langmuir* **1996**, *12*, 6104.
(19) Haggerty, L.; Lenhoff, A. *Biophys. J.* **1993**, *64*, 886.
(20) Ravichandran, S.; Madura, J. D.; Talbot, J. *J. Phys. Chem. B* **2001**, *105*, 3610.

(21) Tilton, R. In *Polymer-Colloid interactions*; Dubin, P., Farinato, R., Eds.; Wiley: New York, 1999; pp 331−363.
(22) Braem, A. D.; Biggs, S.; Prieve, D. C.; Tilton, R. D. *Langmuir* **2003**, *19*, 2736.
(23) Schaaf, P. *Langmuir* **1987**, *3*, 1131.
(24) Dijt, J. C.; Cohen Stuart, M. A.; Hofman, J. E.; Fleer, G. J. *Colloids Surf.* **1990**, *51*, 141.
(25) Dijt, J. C.; Cohen Stuart, M. A.; Fleer, G. J. *Adv. Colloid Interface Sci.* **1994**, *50*, 79.
(26) Braithwaite, G. J. C.; Luckham, P. F. *J. Chem. Soc.* **1996**, *93*, 1409.
(27) Braithwaite, G. J. C.; Howe, A.; Luckham, P. F. *Langmuir* **1996**, *12*, 4224.
(28) Braem, A. Ph.D. Dissertation; Carnegie Mellon University: Pittsburgh, PA, 2001.
(29) Lok, B. K.; Cheng, Y.; Robertson, C. R. *J. Colloid Interface Sci.* **1983**, *91*, 104.
(30) Lok, B. K.; Cheng, Y.; Robertson, C. R. *J. Colloid Interface Sci.* **1983**, *91*, 87.
(31) Axelrod, D. *Rev. Biophys. Bioeng.* **1984**, *13*, 247.
(32) Hlady, V.; Reinecke, D. R.; Andrade, J. D. *J. Colloid Interface Sci.* **1986**, *111*, 555.
(33) Rondelez, F.; Ausserre, D.; Hervet, H. *Annu. Rev. Phys. Chem.* **1987**, *38*, 317.
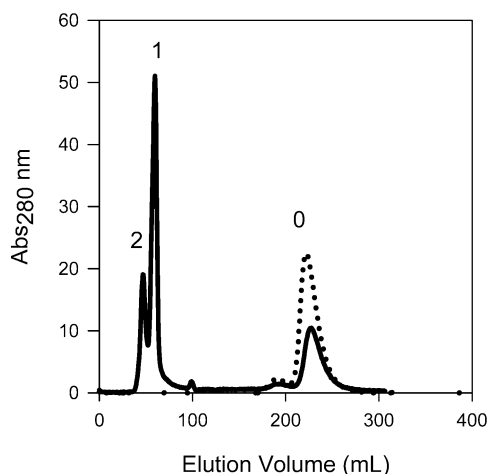
Figure 1. Size exclusion chromatography elution profile of unmodified lysozyme (dashed line) and PEG/lysozyme reaction mixture (solid line). The peak labels correspond to the number of PEG modifications on the lysozyme molecule.

pH 5.1, 100 mM sodium phosphate buffer that contained 20 mM sodium cyanoborohydride. The reaction was allowed to proceed for 17 h at 4 °C. These reaction conditions favor N-terminal modification of the protein.[34,35] PEGylation is not expected to alter the protein secondary structure.[36]

At the end of the reaction period, the PEGylated proteins, unreacted proteins, and unconjugated mPEG-propionaldehyde were separated via size exclusion chromatography on an Äkta Explorer (Amersham Pharmacia) chromatography system, as follows. Prior to sample injection, the Sephacryl S-300 column (1.6 cm inner diameter × 60 cm length) (Amersham Pharmacia) was equilibrated with pH 7.2, 10 mM phosphate buffer containing 150 mM KCl. We injected 2 mL of reaction mixture into the column at a flow rate of 0.5 mL/min and continued the separation at the same flow rate. Upon elution of the PEG/lysozyme reaction mixture from the column, we obtained the chromatogram, based on optical absorbance at 280 nm, shown in Figure 1. Peak 0 corresponds to the elution of unmodified lysozyme from the column, as is apparent from the overlap with the chromatogram for pure unmodified lysozyme. We collected peaks 1 and 2, sending ∼5 mL of the material that eluted between the two peaks to waste so as to limit cross-contamination.

We used MALDI mass spectrometry (PerSeptive Voyager STR) to determine the number of PEG molecules attached to lysozyme in each collected fraction. The sample crystals were prepared in a 3,5-dimethoxy-4-hydroxycinnamic acid matrix. The MALDI-time of flight (TOF) operation conditions were set as follows: the mode of operation was linear, the polarity was positive, the acceleration voltage was 25 000 V, and the delayed extraction time was 750 ns. Analysis of the mass spectra gave mass/charge ratios of 35 500 and 56 200 for peaks 1 and 2, respectively, and 21 300 for the mPEG-propionaldehyde alone. The width of the MALDI peaks was ∼6000 mass/charge (*m/e*) units. Given the 21 300 molecular weight of PEG and the 14 600 molecular weight of lysozyme, the molecular weights of peaks 1 and 2 correspond to mono- and di-PEG-modified lysozyme, respectively. Although we could not follow PEG elution from the size exclusion chromatography (SEC) column via absorbance changes, we did not see a peak at 21 300 in the MALDI profiles of the PEGylated protein fractions, indicating no homopolymer PEG contamination. After size exclusion chromatography, the mono-PEG and di-PEG fractions were concentrated with 3 kDa molecular weight cutoff (MWCO) Centricon Plus filters (Millipore). The concentrated fractions were then dialyzed overnight against the experimental buffer.

It is difficult to determine the location of the PEG modification on the protein, and others have pursued several different experimental strategies toward this aim.[37–39] We attempted to confirm that the location of the PEG modification for mono-PEGylated lysozyme was the N-terminus by subjecting whole proteins and tryptic digests of unmodified and mono-PEGylated proteins to reverse-phase high performance liquid chromatography (HPLC) and MALDI mass spectrometry analysis. We used a reverse-phase C18 column (Waters) to separate lysozyme and mono-PEG—lysozyme. The column was cleaned with acetonitrile for 30 min and then water for 30 min before each experiment. The column was then equilibrated against a 35% acetonitrile solution. We monitored the elution of unmodified and PEGylated protein on a 35–55% acetonitrile gradient over 50 min. We used a 100 μL sample loop and a flow rate of 1 mL/min. Mono-PEG—lysozyme eluted from the column as a single peak, consistent with one primary location for PEG modification.

For tryptic digests, we followed a standard protocol.[4] We reduced lysozyme, mono-PEG—lysozyme, and di-PEG—lysozyme solutions with DTT in 10 mM phosphate buffer, pH 7.2, with 150 mM KCl. We added 42 μL of a 5 mg/mL DTT solution to 100 μL of protein solution (0.06–5 mg/mL). We then added 38 μL of iodoacetate solution (10 mg/mL) to the reduced protein solution. The solutions were incubated at room temperature for 6 h and then dialyzed twice in 8 kDa MWCO tubing (Fisher Scientific) against the phosphate buffer. We then added trypsin to obtain a trypsin/sample mass ratio of 1:30 and incubated at 37 °C overnight.

The HPLC tryptic digest maps for unmodified and PEG-modified protein were similar. We further analyzed the digests with MALDI using an α-cyano-4-hydroxycinnamic acid matrix. A comparison of the ratio of MALDI peaks for digests of unmodified, mono-PEGylated, and di-PEGylated lysozyme suggested that mono-PEGylated lysozyme was primarily N-terminally modified, with slight modification at lysine residues 33 and 97. Di-PEGylated lysozyme was likely modified at the N-terminus and at residue 33, with slight modification at residues 97 and 116.

Size of the PEG—Lysozyme Conjugates. We measured the hydrodynamic diameters of unmodified lysozyme, nominal 20 kDa PEG homopolymer, and PEGylated lysozyme using a Malvern Zetasizer dynamic light scattering apparatus.[40] Malvern's version of the autoCONTIN algorithm was used to fit measured autocorrelation functions to a distribution of decay times, from which a distribution of diffusion coefficients was calculated. Apparent hydrodynamic diameters were calculated from the diffusion coefficients using the Stokes—Einstein equation for spherical particles. Samples were dissolved in pH 7.2, 10 mM phosphate buffer containing 150 mM KCl and filtered with 0.2 μm filters prior to measurement, with results listed in Table 1.

Optical Reflectometry. Details of the optical reflectometry technique, the standard methods of data analysis, and the particular instrument used here have been described elsewhere.[14,21–22,41] Conversion from raw reflectivity data to surface excess concentrations was based on the two-homogeneous-layer striated interface optical model, consisting of the oxide layer and the adsorbed layer separating the semi-infinite solution and the semi-infinite silicon slab. We used values of 0.18 and 0.134 cm³/g for the refractive index increment of lysozyme[18] and PEG,[42] respectively. The amount of material required to measure the refractive index increment of the PEGylated conjugates exceeded that which we could produce economically. Hence, the refractive index increments of the PEGylated conjugates were estimated as 0.154 and 0.146 cm³/g for mono-PEG—lysozyme and di-PEG—lysozyme, respectively, using a mass average of the increments for PEG homopolymer and lysozyme for each conjugate molecule.

(34) Kinstler, O. B.; Gabriel, N. E.; Farrar, C. E.; Deprince, R. B. N-Terminally Chemically Modified Protein Compositions and Methods. U.S. Patent 5,824,784, 1998.

(35) Kerwin, B. A.; Chang, B. S.; Gegg, C. V.; Gonnelli, M.; Li, T.; Strambini, G. B. *Protein Sci.* **2002**, *11*, 1825.

(36) Kinstler, O. B.; Brems, D. N.; Lauren, S. L.; Paige, A. G.; Hamburger, J. B.; Treuheit, M. J. *Pharm. Res.* **1996**, *13*, 996.

(37) Kendrick, B. S.; Kerwin, B. A.; Chang, B. S.; Philo, J. S. *Anal. Biochem.* **2001**, *299*, 136.

(38) Veronese, F. M.; Sacca, B.; Polverino de Laureto, P.; Sergi, M.; Caliceti, P.; Schiavon, O.; Orsolini, P. *Bioconjugate Chem.* **2001**, *12*, 52.

(39) Lee, H.; Park, T. G. *J. Pharm. Sci.* **2003**, *92*, 97.

(40) Chu, B. *Laser Light Scattering*; Academic Press: New York, 1974.

(41) Furst, E.; Pagac, E.; Tilton, R. *Ind. Eng. Chem. Res.* **1996**, *35*, 1566.

(42) Fu, Z.; Santore, M. M. *Macromolecules* **1998**, *31*, 7014.

Table 1. Molecular Weights as Measured by MALDI Mass Spectroscopy and Hydrodynamic Sizing as Determined by Dynamic Light Scattering[a]

	unmodified lysozyme	PEG−lysozyme	di-PEG−lysozyme	PEG
molecular weight (g/mol)	14 600	35 500	56 200	21 300
diffusion coefficient (cm^2/s)	$(1.32 \pm 0.2) \times 10^{-6}$	$(4.4 \pm 0.4) \times 10^{-7}$	$(3.03 \pm 0.3) \times 10^{-7}$	$(6.2 \pm 0.5) \times 10^{-7}$
diameter of equivalent sphere (nm)	3.3 ± 0.4	9.9 ± 0.9	14.4 ± 1.2	6.9 ± 0.5
area/molecule (nm^2)	9.1	77.0	162.9	37.4
dimensions of cylinder (nm)		6.9×10.5		

[a] The error values correspond to the width of the light scattering peak.

For both reflectometry and TIRF experiments, the temperature was held constant at 25 ± 1 °C. Buffer was pumped through the flow cell for at least 30 min prior to baseline collection for all experiments. Adsorption took place in rectangular slit flow cells, with solutions undergoing fully developed laminar flow at a 32 s^{-1} wall shear rate.

TIRF. The basic principles of TIRF[30,43,44] have been described elsewhere. For this study, we used a modular Spex Fluorolog-3 (Jobin Yvon Horiba) fluorescence spectrometer. A TIRF flow cell manufactured by Bioelectrospec was mounted into the spectrometer as described previously.[16] Excitation and emission slit widths were both fixed at 7 nm. We monitored intrinsic tryptophan fluorescence during adsorption at excitation and emission wavelengths of $\lambda_{ex} = 295$ nm and $\lambda_{em} = 320$ nm, respectively. The tryptophan intensity is proportional to the surface concentration of lysozyme only, since PEG does not fluoresce. Hence, we used TIRF to follow the adsorption of lysozyme.

Exchangeability refers to the replacement on the surface of one type of preadsorbed molecule by a different type of molecule that is in solution. We monitor the exchangeability of PEG−lysozyme and unmodified lysozyme by fluorescently labeling unmodified lysozyme with fluorescein isothiocyanate (FITC) and challenging an adsorbed layer of one species with a solution containing the other species. Optical reflectometry measurements show that FITC−lysozyme and unmodified lysozyme are identical with respect to adsorption and reversibility on silica. There is no evidence for labeling-induced artifacts. The FITC labeling procedure for unmodified lysozyme was described previously.[16,18] The fluorescein excitation and emission wavelengths were set to $\lambda_{ex} = 488$ nm and $\lambda_{em} = 520$ nm, respectively.

In the exchange experiments, PEGylated lysozyme was not labeled with FITC but un-PEGylated lysozyme had an FITC label. Thus, the tryptophan emission traces the total protein surface excess concentration, while the FITC emission is a reporter for the un-PEGylated protein.

Because fluorescein fluorescence exhibits pH sensitivity, and therefore electrostatic potential sensitivity, monitoring fluorescein emission during exchange experiments on negatively charged silica surfaces also provides information about the average proximity of the FITC moiety to the surface. Details of the TIRF technique that exploits this phenomenon are provided elsewhere.[16,18] Here, we combine the conventional TIRF exchange experiments with the pH-sensitive fluorophore TIRF approach[18] to monitor reorientation dynamics within the PEG-modified lysozyme layer.

Atomic Force Microscopy. In situ force measurements between adsorbed layers on opposing silica surfaces were performed with a Nanoscope III atomic force microscope (Digital Instruments, now Veeco Metrology). The fluid cell volume was ~0.1 mL, and solutions were manually introduced to the fluid cell by syringe. Force measurements were conducted and analyzed according to well-established procedures developed elsewhere.[26,27] Forces were calculated from the measured cantilever deflection by applying Hooke's law with a predetermined cantilever spring constant. The force curves were normalized by the tip radius of curvature. We used the nominal tip radius and cantilever spring constant as reported by the manufacturer. We considered these approximations to be acceptable because the shapes of the force curves, not the force magnitudes, were used to estimate the adsorbed layer thickness, and results are only compared for measurements made with the exact same cantilever.

(43) Buijs, J.; Hlady, V. *J. Colloid Interface Sci.* **1997**, *190*, 171.
(44) Roth, C. M.; Lenhoff, A. M. *Langmuir* **1995**, *11*, 3500.

Changes in the separation distance were determined directly from the calibrated piezoelectric drive displacement and the measured cantilever deflection. As is customary, we took the onset of the constant compliance regime of the force curve to represent the zero apparent separation distance between the opposing surfaces.[26] This would not necessarily correspond to direct contact between the tip and the substrate, because constant compliance occurs whenever the force gradient exceeds the cantilever spring constant. Hence, some of the protein–polymer conjugate could be trapped between the tip and the substrate at the onset of constant compliance, resulting in uncertainty in the absolute separation distance.

To measure the force between opposing layers of adsorbed mono-PEGylated lysozyme, we injected approximately 20 flow cell volumes of a 0.1 μM solution of mono-PEG−lysozyme into the fluid cell and allowed 1 h for adsorption to both the silica slide and the cantilever tip. We then collected force curves at several different locations on the slide over several hours. After rinsing with buffer, we then replaced the dilute solution with 20 flow cell volumes of a 10 μM solution of mono-PEG−lysozyme and allowed it to equilibrate for 30 min prior to collecting new force curves. We continued to collect force curves at different locations on the slide for the next several hours.

Results and Discussion

Size of the Conjugates. Awareness of the dimensions and structure of the adsorbing protein facilitates the interpretation of adsorption isotherms. The diffusion coefficients and equivalent sphere hydrodynamic diameters are summarized in Table 1. The hydrodynamic diameters of mono-PEGylated and di-PEGylated lysozyme are approximately the sum of the diameters of one lysozyme molecule and one or two PEG chains. The protective effect of PEGylation has been described as originating from a shell of PEG chains surrounding the protein,[11,18] but in the case of mono-PEGylation, it is unlikely that a single 20 kDa chain would be able to surround the protein. The dimensions of the conjugates suggest that the 20 kDa PEG chains exist as relatively unperturbed random coil domains adjacent to the lysozyme molecule, rather than as a protein shroud. Table 1 also lists the cross-sectional area of the equivalent spherical molecule calculated from the hydrodynamic diameter. We used these area-per-molecule values in order to estimate area fractional surface coverages corresponding to different points on the adsorption isotherms below. We also modeled mono-PEG−lysozyme as a cylinder, using the friction coefficient, f,

$$f = 6\pi\eta_0 \frac{L/2}{\ln q + 0.312 + 0.565q^{-1} - 0.100q^{-2}} \quad (1)$$

for a short cylinder, where L is the length of the cylinder and q is the cylinder's aspect ratio (L/D), where D is the diameter of the cylinder, valid for $2 < q < 30$.[46,47] We fixed D as 6.9 nm, or the diameter of an unperturbed PEG coil in solution, and calculated $L = 10.5$ nm from the diffusion coefficient reported in Table 1. The footprint of this cylinder lying with the long axis parallel to the adsorbing surface